Low temperature synthesis of MoS2 and MoO3:MoS2 hybrid thin films via the use of an original hybrid sulfidation technique

Hajar Ftouhi, Hind Lamkaouane, Guy Louarn, Mustapha Diani, Jean-Christian Bernède, Mohammed Addou, Linda Cattin

Version of Record: https://www.sciencedirect.com/science/article/pii/S2468023022003881
Manuscript_5c9376724a25b5593bc4b449b8e778e3

Low temperature synthesis of MoS_2 and MoO_3:MoS_2 hybrid thin films via the use of an original hybrid sulfidation technique

Hajar Ftouhi [(1,2)*], Hind Lamkaouane [(1,3)], Guy Louarn[(1)], Mustapha Diani[(2)], Jean-Christian Bernède [(4)], Mohammed Addou [(2)], Linda Cattin [(1)]

1- Université de Nantes, Institut des Matériaux Jean Rouxel (IMN), CNRS, UMR 6502, 2 rue de la Houssinière, BP 92208, 44000 Nantes, France
2-Équipe de Recherche Couches Minces et Nanomatériaux – Faculté des Sciences et Techniques, Université Abdelmalek Essaâdi, BP 416, Tanger, Maroc
3- Laboratory of Physics of Condensed Matter and Renewable Energy, Faculty of Sciences and Technology, Hassan II University of Casablanca B.P 146, Mohammedia, Maroc
4- Université de Nantes, MOLTECH-Anjou, CNRS, UMR 6200, 2 rue de la Houssinière, BP 92208, 44000 Nantes, France

Abstract

In this study, an original hybrid technique based on rapid thermal annealing (RTA) and chemical vapor deposition (CVD) was used to synthesis MoS_2 and MoO_3:MoS_2 hybrid thin films at low temperature on indium tin oxide (ITO). We show that using the annealing temperature, the annealing duration and the sulfur partial pressure as parameters, it is possible to switch from MoO_3 (20-25nm) to MoS_2 directly without any intermediate compositions. The XPS analysis revealed a complete sulfidation at 380 °C without any deterioration of the ITO conductivity. Then, we synthesized thinner hybrid films (3nm) of MoO_3:MoS_2 in order to be used as anode buffer layer (ABL) in planar organic solar cells (PHJ-OPVs). We have demonstrated that the hybrid ABLs that appear best suited for use in PHJ-OPVs are those with high MoO_3/MoS_2 molecular ratio which have been treated around 210 °C. The introduction of the hybrid ABL with 5% of MoS_2 in the PHJ-OPVs based Aluminum Phthalocyanine Chloride and Fullerene leads to a significant improvement of the OPV efficiency from 1.29 % to 2.49%, this was explained by the complimentary advantages of MoO_3 and MoS_2.

Keywords: Molybdenum disulfide (MoS_2); Hybrid layer (MoO_3:MoS_2); Organic photovoltaic cells; Hole transporting layer; Planar heterojunction.

Corresponding author: hajarftouhi2@gmail.com

1. Introduction

At the end of the last century, numerous research works were dedicated to transition metal dichalcogenides (TMDs). Indeed their photoconductive properties made them promising candidates for the realization of photovoltaic cells. A photovoltaic cell, using WSe_2 single-crystal as absorbing layer, had achieved an efficiency of 17.5% [1]. However, after several years dedicated to obtaining photoconductive TMD layers, it was necessary to admit that these were inoperative to make photovoltaic cells. Actually, it was shown that MX_2 layer, with M = Mo or W and X = S or Se, were photoconductive after high temperature annealing (1073 K) only in presence of Ni [2][3]. Unfortunately, Ni acts as a catalyst and segregates at the end of the annealing, which causes it to bypass the MX_2 layers, what means that all attempts to build photovoltaic cells have failed.

More recently, following the enthusiasm aroused by the isolated graphene in 2004 [4], a considerable resurgence of interest in TMDs has appeared, for indeed, like graphene, they are bi-dimensional with a 2D structure [5][6]. There was renewed interest in two-dimensional (2D) materials such as TMDs due to their suitability for future applications in optoelectronic devices [7] [8]. In particular, molybdenum disulfide (MoS_2) was proposed as a hole transporting layer (HTL) in hybrid dye photovoltaic cells (DSSC) [9] and organic photovoltaic cells (OPVs) [10][11]. It was also used as anode in lithium batteries where it can be substituted to graphite due to its higher specific capacity [13]

MoS_2 crystallizes in a lamellar structure. In this two-dimensional material, the atoms forming the S-Mo-S sandwiches are strongly bound, while the sandwiches themselves are weakly coupled to each other by weak Van Der Waals forces (Figure 1). These van der Waals plans are chemically inert without dangling bonds.

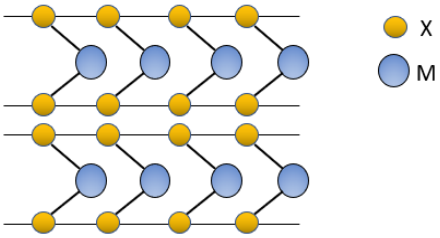

Figure 1– Schematic diagram of MX_2

The fact that MoS_2 is chemically inert induces that it can be used in many applications. Thus it can be used as a lubricant [14] in transistors [8][15], as catalysts [16] and, as discussed above, batteries [13] and OPVs [10] [11] [17] [18]. MoS_2 has an indirect band gap of 1.30 eV and a direct band gap of 1.85 eV. These values are bulk values, but, in the case of ultrathin layer, it increases and it is 1.8 eV for a monolayer [7] [19]. Carrier mobility is quite high for instance a mobility of 200 $cm^2\ V^{-1}\ s^{-1}$ in single layer has been reported [20]. In the

case of MoS_2 monolayer electron mobility values are widely spread across three orders of magnitude (1-1000 $cm^2\ V^{-1}\ s^{-1}$) [7].

All that makes that, if, as said above, MoS_2 has been probed unsuccessfully as absorbing layer in photovoltaic cells, today it is back, but as HTL in OPVs [10] [11] [17] [18]. If many techniques such as mechanical exfoliation [21], sputtering [22] pulsed laser deposition [25], chemical vapor deposition [26], sol-gel fabrication [23] and electrochemical processes [18] were used to obtain MoS_2 thin layers, these techniques are not so easy to integrate into the process of making cells which excludes any use of heat treatment at a high temperature and any technique that risks to deteriorate the properties of organic materials. Moreover, due to specific properties of MoS_2 and MoO_3, such as band structure, it appears that, instead of using a pure layer of MoS_2, it is better to use a MoO_3:MoS_2 hybrid layer as HTL [18]. In fact, if MoO_3 is known to be an excellent hole extractor, its band structure is not ideal for blocking electrons, but that of MoS_2 makes it an excellent electron blocker, but not a good hole extractor. Hence the idea of a hybrid layer that allows to combine the positive effects of the both materials [18]. Actually, such idea has been already probed through PEDOT:PSS-MoS_2 [24] and MoO_3:MoS_2 hybrid HTL [11]. We have already shown that such MoO_3:MoS_2 hybrid HTL when deposited by electrochemistry is efficient but it needs a quite complicated post-deposition technique [18]. In the present work, we demonstrate that it is possible to grow MoO_3:MoS_2 hybrid HTL and MoS_2 layers with a simpler and reproducible technique, using a moderated annealing temperature under partial S atmosphere. Starting from MoO_3 thin films deposited by sublimation under vacuum, we show that, using the annealing temperature and the sulfur partial pressure as parameters, it is possible to switch from MoO_3 to MoS_2, but also to sweep all the intermediate compositions for the hybrid layer. Then, MoO_3:MoS_2 hybrid layers were introduced as HTL in OPVs based on AlPcCl/C_{60} organic planar heterojunction. It is shown that this HTL improves significantly the power conversion efficiency.

2. Experimental details : Methods and techniques

2.1. MoS_2 and MoO_3:MoS_2 thin films synthesis

We have used ITO coated glass substrates provided by SOLEMS, while the chemical products were provided by CODEX International. After cleaning and heating the substrates during 10 min at 100°C, they were introduced into the vacuum chamber. When a vacuum of 10^{-4} Pa was achieved, MoO_3 was sublimated from a tungsten boat; the deposition rate and the layer thickness were measured in-situ using a quartz microbalance. Then the sample was introduced into the sulfidation apparatus, which consists in a vacuum apparatus equipped with an oven specifically designed for thin film sulfidation (Figure 2). When a vacuum of 10^{-4} Pa is achieved, we proceeded to the MoO_3 sulfidation through the process summarized in scheme 1.

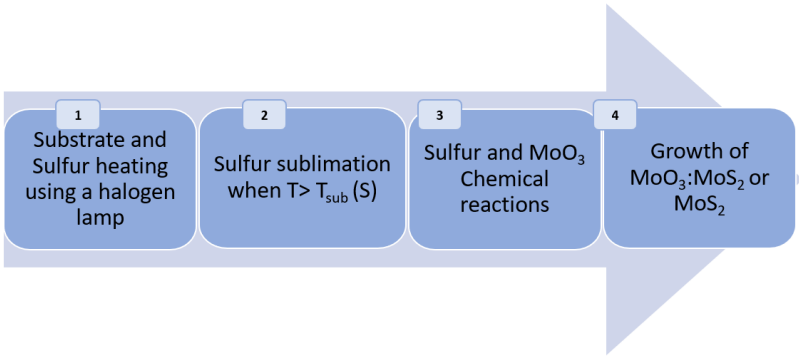

Scheme 1– Schematic diagram for the sulfidation process steps

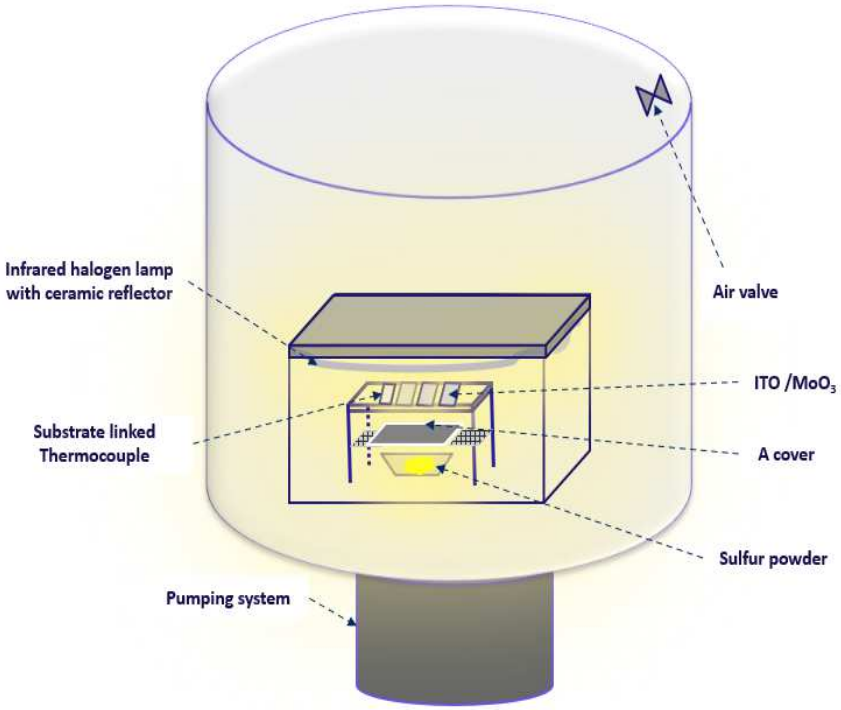

Figure 2– Laboratory made sulfidation apparatus.

The vapor pressure of sulfur is very high, it vaporizes at 150°C, so substrate heating is sufficient for vaporizing sulfur. The reference temperature during the process was the temperature measured with a thermocouple stuck to an ITO coated glass substrate. This annealing temperature, the annealing duration and the partial sulfur pressure, were used as parameters to manage the final sulfidized film properties. The technique that has been developed in our laboratory to handle the production of MoS_2 from MoO_3 thin films is a hybrid technique, that is to say a combination between two known thin layer deposition techniques: rapid

thermal annealing (RTA) and chemical vapor deposition (CVD) and we called it RTA-CVD. The RTA-CVD technique helps to reduce unwanted reactions that can lead to the formation of unexpected particles.

2.2. Organic solar cells realization

In the present work, OPVs were based on planar heterojunctions (PHJ), based on small organic molecules deposited under vacuum. Due to the ease in controlling the thickness and morphology of the organic material this technique allows obtaining reproducible results. These OPVs are classically based on an organic bilayer, which consists of an electron donor/electron acceptor pair (ED/EA), sandwiched between two electrodes. About electrodes, The reflexive cathode is an aluminum layer, while the transparent conductive anode is an indium tin oxide (ITO) layer, coating the glass substrate [28]. Moreover, in order to achieve OPVs with good efficiency, it is necessary to insert buffer layer between electrodes and organic layers. The buffer layer between the aluminum cathode and EA, a thin Alq_3 (Tris-(8-hydroxyquinoline) Aluminum) film, is introduced as electron transporting layer [29]. The hole transporting layer (HTL), between the anode and the ED, is the MoO_3:MoS_2 hybrid buffer layer synthesized following the process described above. The ED/EA couple used during this study was the well-known couple AlPcCl/C_{60}. Therefore, the OPVs studies were as follows:

ITO (100 nm)/MoO_3:MoS_2 (3 nm)/AlPcCl (26 nm)/C_{60} (45 nm)/Alq_3 (9nm)/Al (100 nm), the different thicknesses and deposition rates were optimized in previous publications [30]. It must be noted that the aluminum top electrodes were thermally deposited, using a mask, which gives an effective active area of 0.10 cm^2.

2.3. Characterization techniques

The surface morphology of the different films was visualized using a scanning electron microscope (SEM) (Centre de microcaractéristion, Institut des Matériaux Jean Rouxel, Université de Nantes) with a field emission scanning electron microscope (JSM JEOL 7600F). The composition of the films has been studied by energy dispersive spectrometry (EDS) with a BRUKER Quantax silicon drift detector (SDD) mounted to the SEM by visualizing the cross section of films we were able to check precision of the thickness given by the quartz monitor.

Root-Mean-Square roughness (RMS) was estimated using an atomic force microscope (AFM). AFM images of the films were taken ex-situ at atmospheric pressure and room temperature. All measurements have been performed in Tapping Mode™ on a MultiMode8 SPM AFM (Bruker). A crystal silicon probe of type TESPA (NanoWorld) with an imaging resonance frequency around 320 KHz was used. The elastic coefficient was

40 N/m, the scanning frequency is 1 Hz. The obtained AFM images were analyzed with Gwyddion 2.58 software, which is mainly used for statistical analyses of surface characteristics.

The optical absorption was measured from 300 nm to 1200 nm using a UV/visible spectrometer (PERKIN ELMER Lambda 1050 spectrophotometer).

The chemical stats of the prepared films were examined using X-ray photoelectron spectroscopy (XPS) measurements were carried out at room temperature on an Axis Nova spectrometer (Kratos Analytical) using the Al Kα line (1486.6 eV) as the excitation source. Survey spectra were acquired at pass energies of 80 eV (energy resolution of 0.87 eV). Data analysis was performed using CasaXPS software. Binding energy for the C_{1s} hydrocarbons peak was set at 284.8 eV in the calibration procedure. The core level spectra were acquired with an energy step of 0.1 eV and using a constant pass energy mode of 20 eV, (energy resolution of 0.48 eV). The quantitative studies were based on the determination of the Mo_{3d}, S_{2p}, and O_{1s} peak areas with 3.32, 0.66, and 0.78 sensitivity factors, respectively. These values were provided by the manufacturer.

Photoelectron Spectroscopy in Air (PESA) was used to measure the work function, W_F, of different HTLs. The PESA technique is based on the fact that when a sample surface is bombarded with a slowly increasing amount of ultraviolet photon energy, photoelectrons start to emit at a certain energy level. This energy level corresponds to W_F. When the photoelectron output is plotted on an X/Y axis, with horizontal axis as the UV energy applied, and the vertical axis as the standardized photoelectron signal, it is possible to draw a line from which it is possible to deduce the C value of the sample.

Raman spectra were recorded on a Renishaw InVia reflex spectrometer (λ_{exc} = 514.5 nm) and Jobin-YvonLabram HR800 UV (λ_{exc} = 325 nm). All experiments were carried out at room temperature, in air on thin films freshly deposited on a silicon wafer. The recorded data frequently showed a pronounced baseline coming from the silicon substrate, due to of the very thin thickness of the film under interest (MoO_3 and MoS_2).This is the reason why we also worked with a UV laser (Helium-Cadmium Laser) in order to better characterize the surface layer, at the expense of the substrate.

3. Experimental results

3.1 From MoO_3 to MoS_2 thin films

We have already shown that, starting from Mo thin films it is possible to synthesize MoS_2 thin films by sulfidation [31]. The morphology of the obtained MoS_2 thin film depends significantly on the experimental conditions, mainly from the annealing temperature used during the sulfidation. Porous and inhomogeneous films were obtained for sulfidation at 300°C, while homogeneous compact films were obtained at 500°C. Such high temperature is not compatible with films deposited onto ITO, because, under S partial pressure,

ITO at 500 °C loses its conductive properties. In the present study, the starting film was a MoO_3 film deposited on ITO and not a Mo film. The MoO_3 deposited by sublimation were amorphous and slightly oxygen deficient ($MoO_{2.7}$). We started with quite low sulfidation temperature, T_s = 300 °C and we increase T_s until we get layers of MoS_2. MoO_3 layers were deposited by sublimation under vacuum (10^{-4} Pa), the deposition rate and the film thickness were measured by a quartz monitor. During the first part of the study dedicated to the synthesis of MoS_2 film from MoO_3 films, the thickness of the MoO_3 films was 20 nm- 25 nm and the MoO_3 deposition rate was 0.05 nm/s. The vacuum before sulfidation was $P_v = 10^{-4}$ Pa and during the annealing it was $P_{Sulfur} = 10^{-2}$ Pa. So, as to keep the process short we have limited the sulfidation time to 10 min.

In order to check the efficiency of our sulfidation process we first proceeded to XPS analysis, a summary of the obtained results is presented in Table 1, while typical XPS spectra are shown in Fig. 3.

Sulfidation temperature (°C)	**300**	**320**	**340**	**360**	**380**
MoS_2 (%)	64	65	81	93.5	100
MoO_3 (%)	36	35	19	6.5	0
(MoS_2)/(MoO_3) Percentage ratio	1.8	1.85	4.25	14	-

Table 1. Influence of the sulfidation temperature on the composition of the MoO_3:MoS_2 films

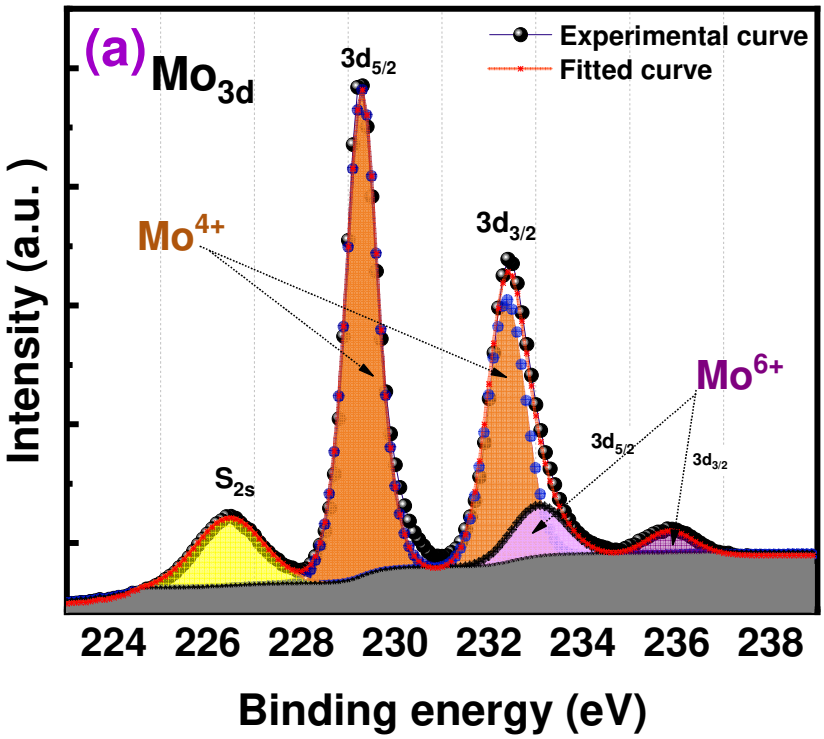
(a)
Mo3d
3d5/2
3d3/2
Mo4+
Mo6+
S2s
3d5/2
3d3/2
Experimental curve
Fitted curve
Intensity (a.u.)
224
226
228
230
232
234
236
238
Binding energy (eV)

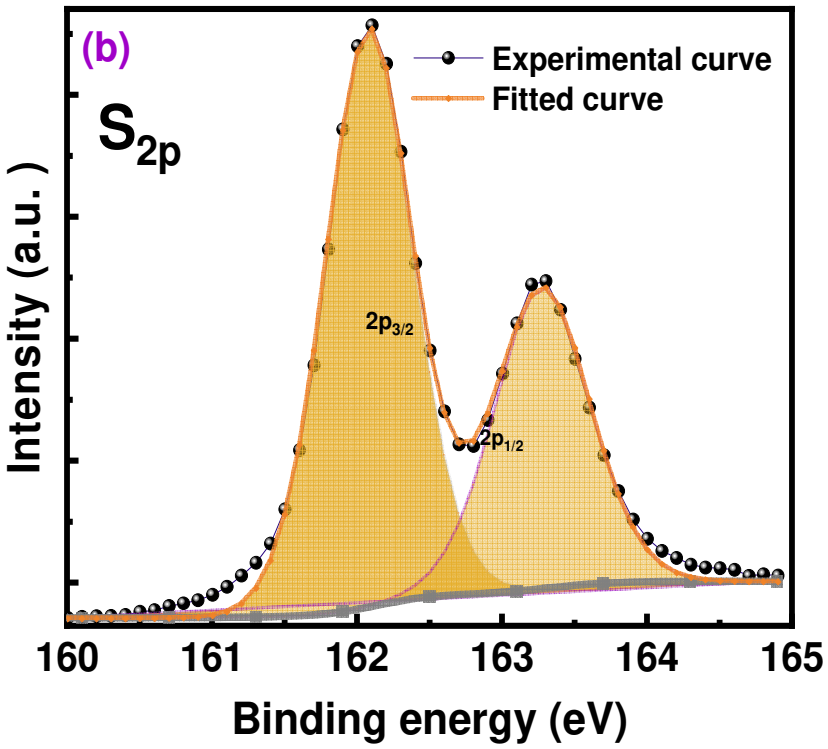
(b)
S2p
Experimental curve
Fitted curve
2p3/2
2p1/2
Intensity (a.u.)
160
161
162
163
164
165
Binding energy (eV)

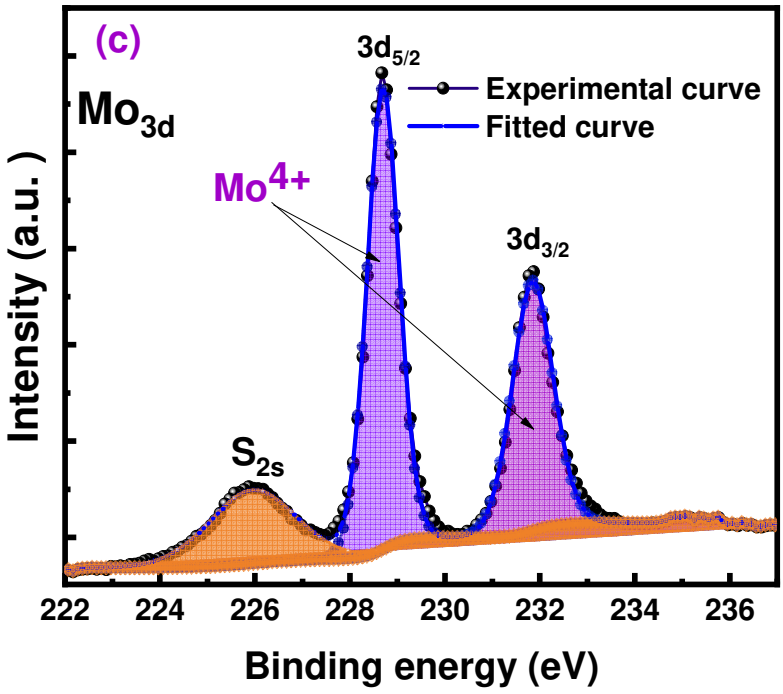
(c)
Mo3d
3d5/2
Experimental curve
Fitted curve
Mo4+
3d3/2
S2s
Intensity (a.u.)
222
224
226
228
230
232
234
236
Binding energy (eV)

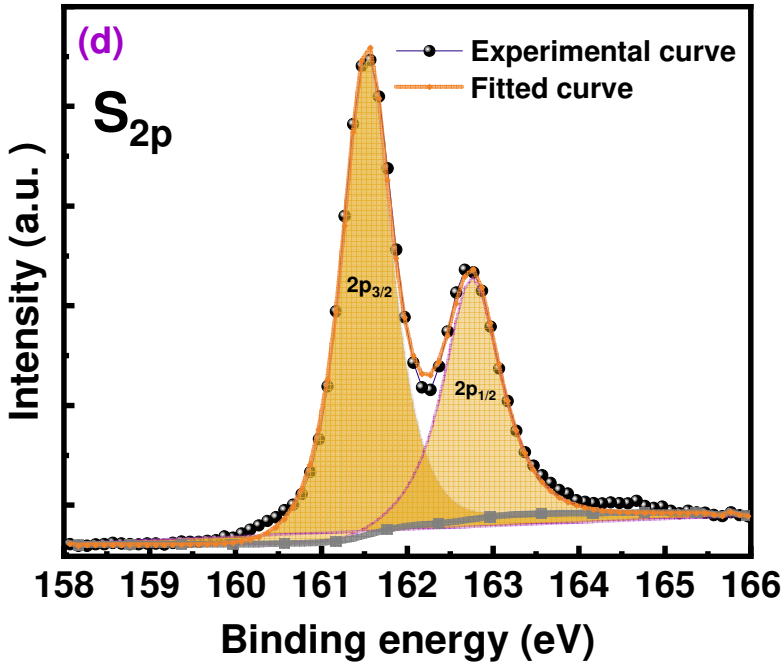

Figure 3 — Typical XPS spectra of MoO_3 films sulfurized at 340°C (a, b) and 380°C (c,d) under sulfur partial pressure.

It can be seen in table 1 that for temperature up to 320°C, the sulfidation is far to be complete, beyond this temperature the percentage ratio $(MoS_2)/(MoO_3)$ ratio increases rapidly, to be complete at 380°C. Before going further into our study we checked that the MoO_3:MoS_2 layer obtained was homogeneous. We have proceeded to microprobe mapping of visualized surfaces. An example of obtained results, coupled with SEM image, are reported in the supporting information S1 for a MoO_3:MoS_2 film sulfurized **at 300°C**. It is clear that Mo, O and S elements are evenly distributed in the layer, which testifies that the MoO_3:MoS_2 hybrid layers are homogeneous.

In the case of the film synthesized at 340°C, i.e. for significant but partial sulfidation, the Mo_{3d} doublet corresponds to, at least, two contributions (**Figure 3a**). If the peak at 226.4 eV corresponds to S(2s) [11, 32, 33], it is necessary to use two doublets to reflect the Mo_{3d} spectrum. The more intense, with $Mo(3d_{5/2})$ and $Mo(3d_{3/2})$ situated at 229.3 eV and 232.4 eV respectively, corresponds to Mo^{4+}, *i.e.* to MoS_2, while the second doublet, situated at 233 eV and 236 eV must be attributed to MoO_3 [11, 32]. For the MoS_2 film synthesized at 380°C **(Figure 3c)** there is only one Mo_{3d} doublet, which corresponds to MoS_2. On the other hand, in

Figure 3 b, d, the doublet S(2p) is clearly resolved, with S($2p_{3/2}$) situated at 162.1 eV and (S$2p_{1/2}$) at 163.3 eV, which corresponds to S^{-2} only, *i.e.* to MoS_2 [20]. Therefore, it is possible to obtain pure MoS_2 films by sulfidation of MoO_3 thin films at 380°C for 10 min, under partial sulfur pressure, $P_{Sulfur} = 10^{-2}$ Pa.

The surface visualization by SEM, of the films before and after sulfidation is presented in **Figure 4**. It can be seen that before sulfidation the MoO_3 films are quite homogeneous with small grains distributed all over the surface, while after sulfidation at 380°C smaller grains are visible at the surface of MoS_2 films. Nevertheless, the MoS_2 films exhibit some disturbed lines or wrinkles which could be a sign of strain in the films. Possibly after annealing and the subsequent cooling, the thermal expansion mismatch between the substrate and the layer left the films under tensile strain.

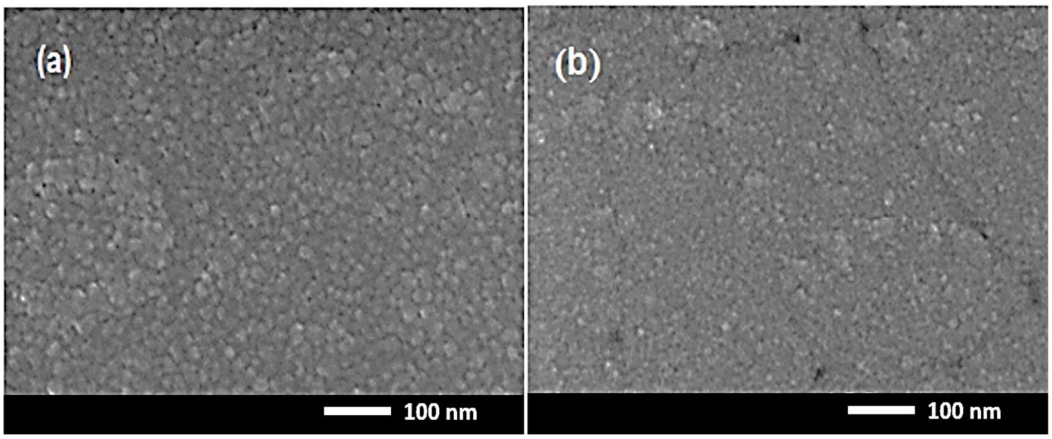

Figure 4– Surface visualization of a MoO_3 film not sulfidized (a) and MoO_3:MoS_2 film sulfidized at 380°C (i.e. a MoO_3:MoS_2 hybrid film) (b)

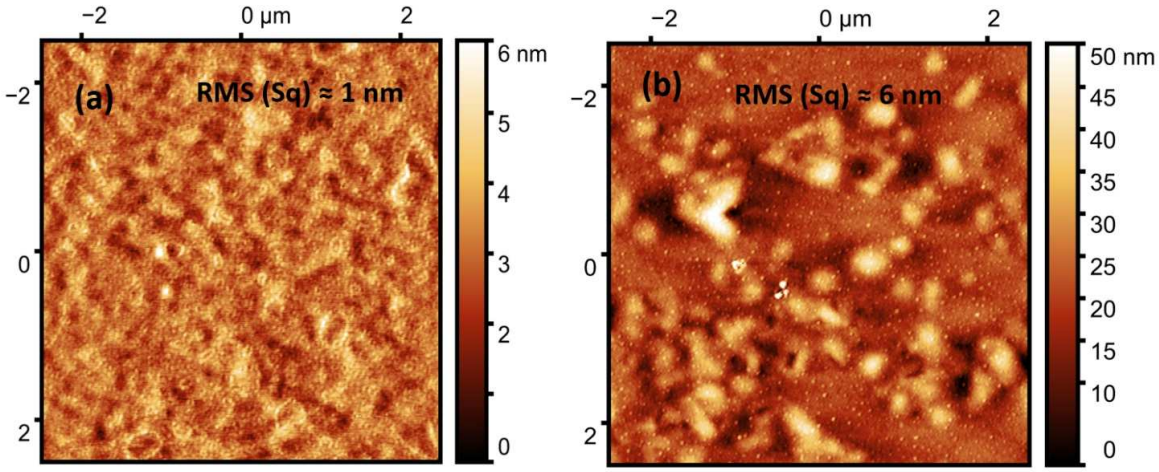

Figure 5– AFM images of a MoO_3 film not sulfidized (a) and of a MoO_3 film sulfidized at 380°C (i.e. a MoO_3:MoS_2 hybrid film) (b)

AFM micrographs (5 x 5 μm^2) of MoO_3 and MoS_2 films are visible in Figure 5, the RMS are 1nm for MoO_3 and 6 nm for MoS_2 films. The increase in the RMS in the case of MoS_2 films may be due to the thermal annealing effect which contribute to grain growth during the sulfidation process.

The absorbance of the films is shown in **Figure 6**. While the spectrum of amorphous MoO_3 film is featureless, two absorption peaks are clearly visible in the absorbance spectra of the others films, mainly in the case of MoO_3 sulfidized at 380°C. By comparison with a single crystal [33], these two contribution peaks may be identified as the excitonic transitions A and B. It must be noted that such excitonic contribution to absorption spectra is generally seen in high quality MoS_2 at 1.945 eV and 2.137 eV respectively [34].

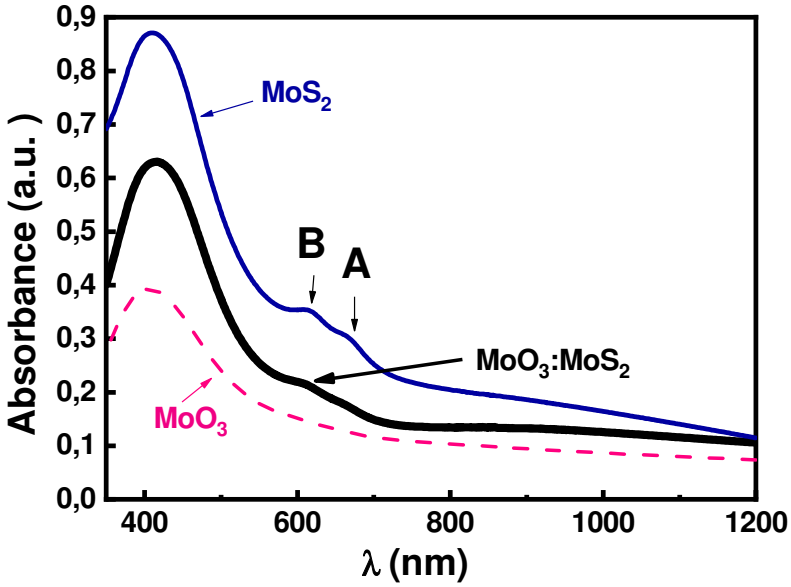

Figure 6– Absorbance spectra of MoS_2 thin film after sulfidation at 380°C (thin line), MoO_3:MoS_2 sulfidized 5 min at 210°C (thick line) and of MoO_3 film before sulfidation (dotted line). The measurements are done using the "3DWB det" module and by subtracting the absorbance of the ITO substrates.

It means that the sulfidation temperature needed to obtain homogeneous and high quality MoS_2 thin films from MoO_3 is smaller than that necessary when the starting layer is Mo. It must be noted that after synthesis of MoS_2 film from MoO_3 deposited on ITO, there is no degradation of the ITO conductivity even for sulfidation at 380°C. This allows us to use this synthesis process for the grow of hybrid HTL in OPVs.

Therefore, building on these results, we studied the case of thin layers of MoO_3 whose thickness corresponds to that used for HTL in cells. Of course, other uses can be considered for these layers of MoS_2, but in this work we will focus the rest of our study on the optimization of MoO_3:MoS_2 hybrid layers for application as a HTL in OPVs.

3.2 MoO_3:MoS_2 thin films as future hybrid HTLs

The following part being dedicated to the realization of a performing HTL, we used a layer of MoO_3 thick of 3 nm, knowing that this thickness allows to obtain good results. Therefore, the starting layer was a MoO_3 film thick of 3 nm deposited onto ITO. Here, the goal is to obtain MoO_3:MoS_2 hybrid layers. Since we have shown that MoO_3 layers thick of 20 nm are partly sulfidized after annealing at temperatures around 300°C, we started this part of the study by using 300°C for 10 min as sulfidation conditions for MoO_3 layers thick of 3 nm deposited on ITO, the partial S pressure being 10^{-2} Pa. The hybrid layers to be used in OPVs, it was important to know their composition, therefore we first proceeded to XPS analysis.

First of all, we have studied a MoO_3 film. The XPS spectra are shown in **Figure 7**.

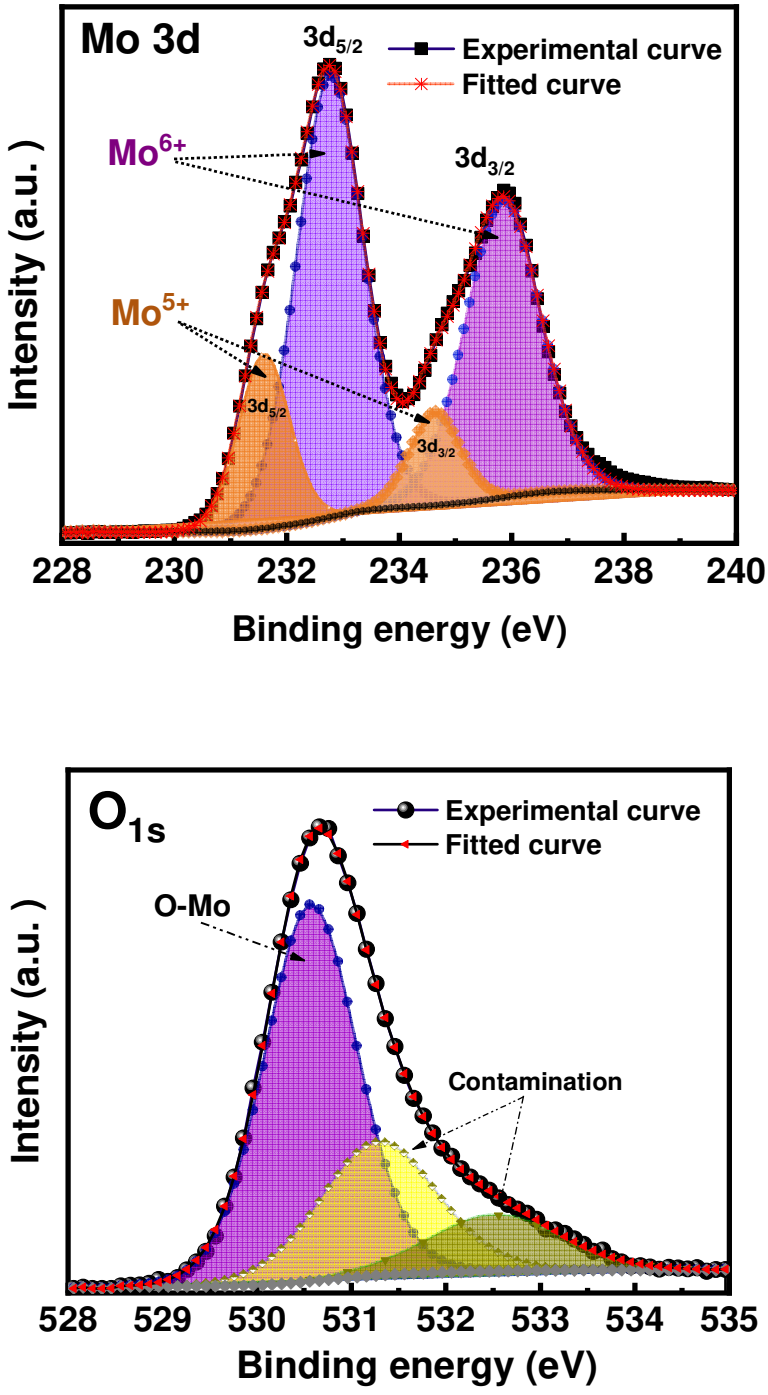

Figure 7– Mo_{3d} and O_{1s} XPS spectra of a MoO_3 thin film (3 nm).

Each component of the Mo3d spectra is clearly asymmetric. It means that the spectrum corresponds to two Mo3d doublets. The main one, situated at 232.8 eV and 235.9 eV corresponds to $Mo3d_{3/2}$ and $Mo3d_{5/2}$ of MoO_3 (Mo^{6+}). The second one, at 231.6 eV and 234.7 eV can be attributed to Mo^{5+} [11]. This last contribution corresponds to 30% of the whole signal. Such result is not unexpected, it is known that the MoO_3 layers deposited by sublimation from a heated powder are systematically oxygen deficient. In the present work an EDS estimation of the MoO_3 films composition has shown that the chemical formula of the deposited layer corresponds to $MoO_{2.7}$. Three contributions are visible in the spectrum of O(1s), the main one, situated at 530.6 eV, must be attributed to MoO_3, while the two others contributions (531.3 eV and 532.5 eV) correspond to surface contamination. It must be noted that, the MoO_3 film deposited onto In_2O_3, being quite thin, 3 nm, the O_{1s} peak situated at 530.6 eV corresponds to not only MoO_3 but also to In_2O_3.

Then, we started the study of MoO_3:MoS_2 hybrid layers using the following process. MoO_3 layers, deposited on ITO by sublimation under vacuum and thick of 3 nm were introduced into the sulfidation apparatus where they were submitted to an annealing at 300°C for 10 min, under S partial pressure ($P_{Sulfur} = 10^{-2}$ Pa). The XPS spectra of such hybrid layers are shown in **Figure 8**.

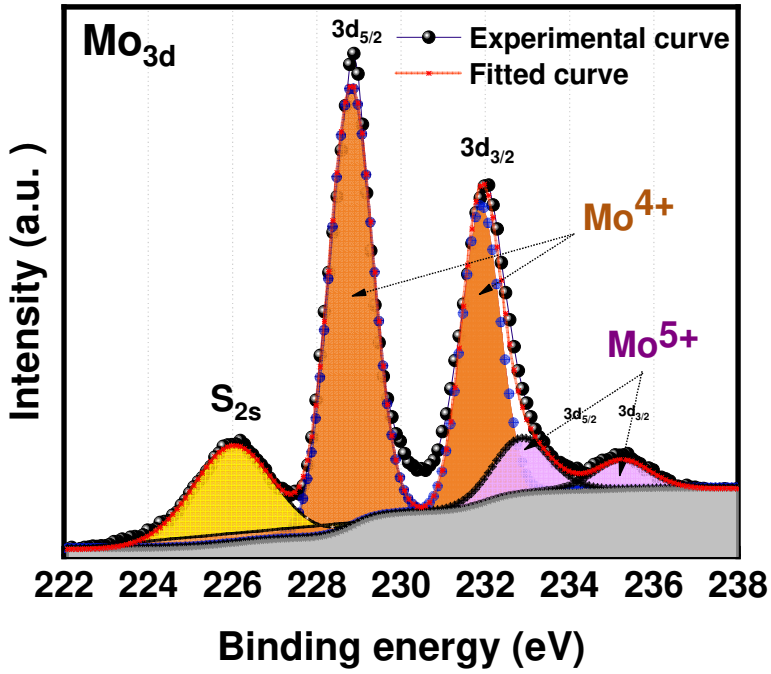

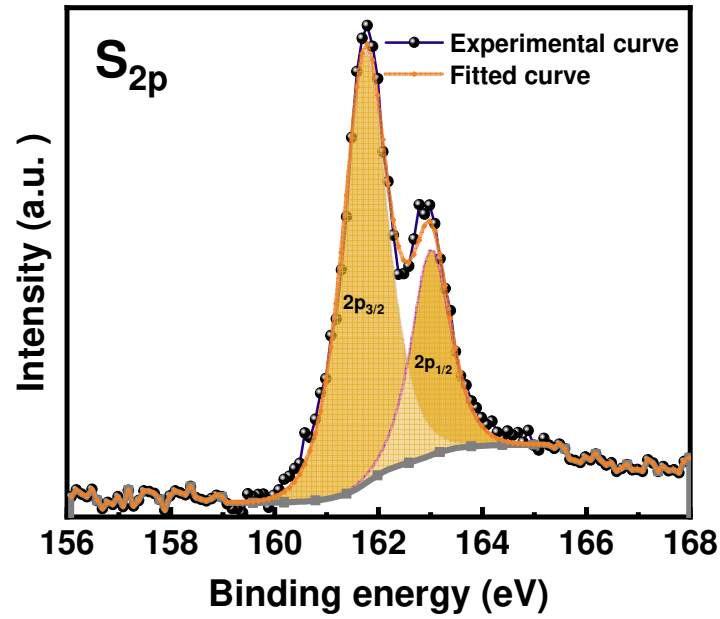

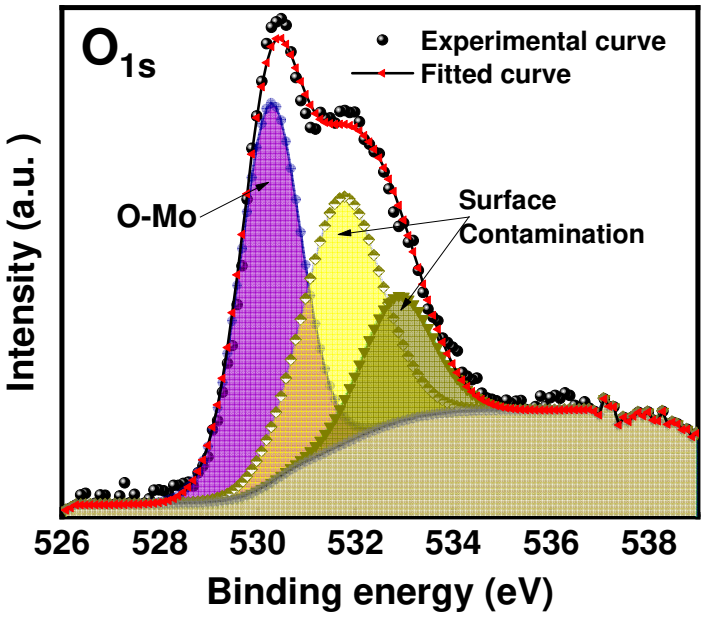

Figure 8 – Mo_{3d}, S_{2p} and O_{1s} XPS spectra of MoO_3:MoS_2 hybrid layer (3 nm) obtained after annealing 10 min at 300°C.

As discussed above, The Mo_{3d} doublet with $Mo(3d_{5/2})$ and $Mo(3d_{3/2})$ situated at 228.9 eV and 232.0 eV respectively, corresponds to MoS_2, while the second smaller one, situated at 232.9 eV and 235.5 eV must be

attributed to MoO_3. On the other hand the S_{2p} doublet (161.75 eV, 163.0 eV) corresponds to MoS_2, while the O_{1s} peak situated at 530.4 eV corresponds to M-O (M = Mo and In, the small thickness of the hybrid layer induces the detection of In_2O_3) and the others contributions correspond to surface contamination. If a MoO_3:MoS_2 hybrid layer is obtained, there is less than 10 at.% of MoO_3 for more than 90 at.% of MoS_2. When such hybrid layer was introduced as HTL in PHJ-OPVs the results were quite bad. Actually, MoO_3 being the hole extracting layer, it must be dominant in the MoO_3:MoS_2 hybrid layer. It appears from preliminary results that the molecular ratio MoO_3/MoS_2 must be greater than or equal to 5. Therefore, we have modified the sulfidation protocol, the duration of the annealing was reduced to 5 min and we have progressively reduced the annealing temperature.

In **Figure 3** and **8** the MoO_3 contribution represents less than 10% of the Mo_{3d} signal, so, for the simplicity of deconvolution of the Mo_{3d} doublet, as the binding energy of Mo^{5+} it is close to that of Mo^{6+}, we have included these 2 components in a single contribution.

Annealing temperature (°C)	**300**	**280**	**250**	**220**	**210**	**190**	**160**
MoS_2 (%)	90	60	15	8	5	3	1
MoO_3 (%)	10	40	85	92	95	97	99
MoS_2/MoO_3 Percentage ratio	0.11	0.66	5.66	11.5	19	32.33	99

Table 2– Influence of the sulfidation temperature on the composition of the MoO_3:MoS_2 hybrid HTL layers, (Sulfidation parameters others than the temperature: duration 5 min and partial sulfur pressure, $P_S = 10^{-2}$ Pa).

We have seen that, in MoO_3 thin films they are two oxidation states for Mo, Mo^{6+} corresponding to MoO_3 itself and Mo^{5+} due to oxygen vacancy in the MoO_3 film. Nevertheless these two oxidation states pertain to MoO_3 thin films. Therefore, in **Table 2**, for calculating the molecular ratio MoO_3/MoS_2 we have added these two contributions to estimate the MoO_3 percentage, while the MoS_2 contribution corresponds to Mo^{4+}. It must be noted that the ratio Mo^{6+}/Mo^{5+} is stable whatever the sulfidation conditions are. It means that the presence of Mo^{5+} is not at the origin of the sulfidation reaction. The presence of Mo^{5+} in the hybrid HTL after sulfidation is positive for their use in OPVs because it was shown that presence of oxygen vacancies increases J_{sc}, due to the fact that these vacancies open a path for carrier transfer via gap states induced by these vacancies [35, 36].

From **Table 2** it can be deduced that the MoO_3:MoS_2 hybrid layers that appear best suited for use in OPVs, *i.e.*, those with sufficiently high MoO_3/MoS_2 molecular ratio, are those that have been treated at a temperature between 250 and 190°C.

The spectra of a MoO_3:MoS_2 hybrid layer after annealing 5 min at 220°C, which composition allows using it as HTL in OPV are shown in **Figure 9**. We can see clearly the three Mo(3d) contributions, Mo^{6+} , Mo^{5+} ,due to MoO_3, and Mo^{4+} , due to MoS_2, the contribution to MoS_2 being notably smaller than that encountered in **Figure 8**. On the other hand, the S(2p) doublet can be attributed to MoS_2, while the main contribution to the O_{1s} corresponds to metal oxide.

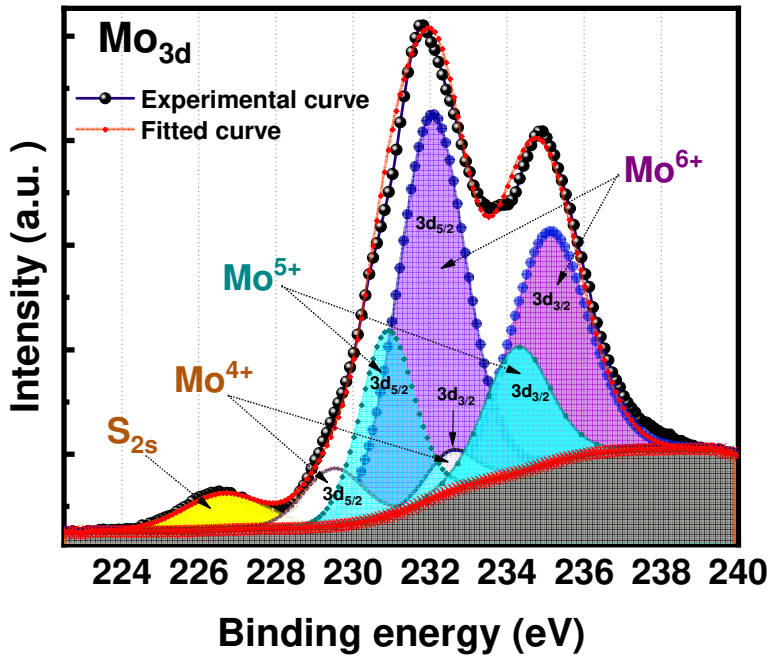

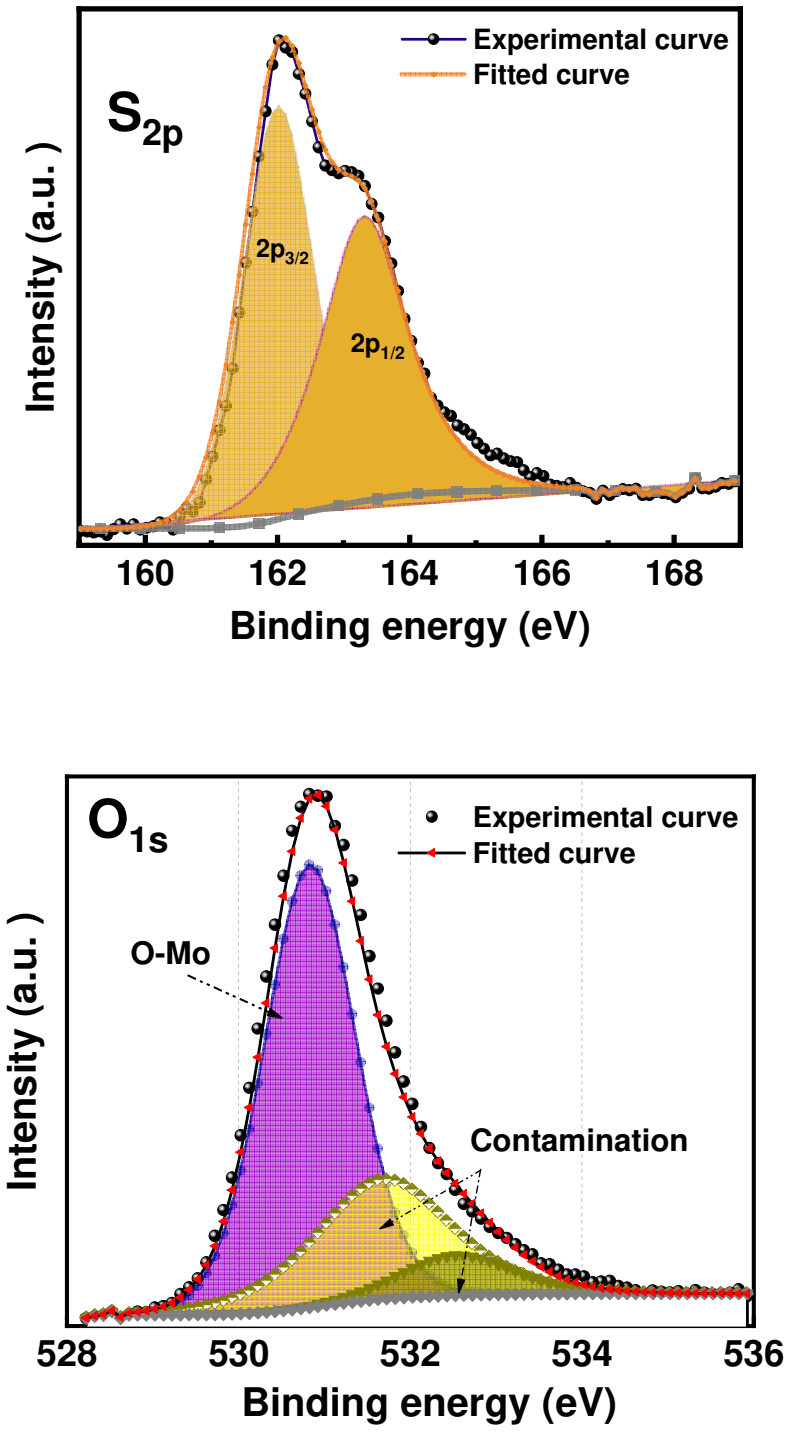

Figure 9– Mo3d, S2p and O1s XPS spectra of MoO_3:MoS_2 hybrid layer obtained after sulfidation 5 min at 220 °C.

An AFM image of the MoO_3:MoS_2 hybrid layer obtained after sulfidation 5 min at 220 °C is presented in **Figure 10**. Many small grains are clearly visible. Some seem to form small circles probably initiated by some small inhomogeneities present on the surface of the layers. The RMS of these hybrid layers was estimated to be around 1 nm. This RMS corresponds to the RMS of the ITO film, which means that the 3 nm thick hybrid HTL does not modifies significantly the morphology of the anode of the OPVs. Moreover such small RMS is positive for their use in OPVs because it avoids leakage current.

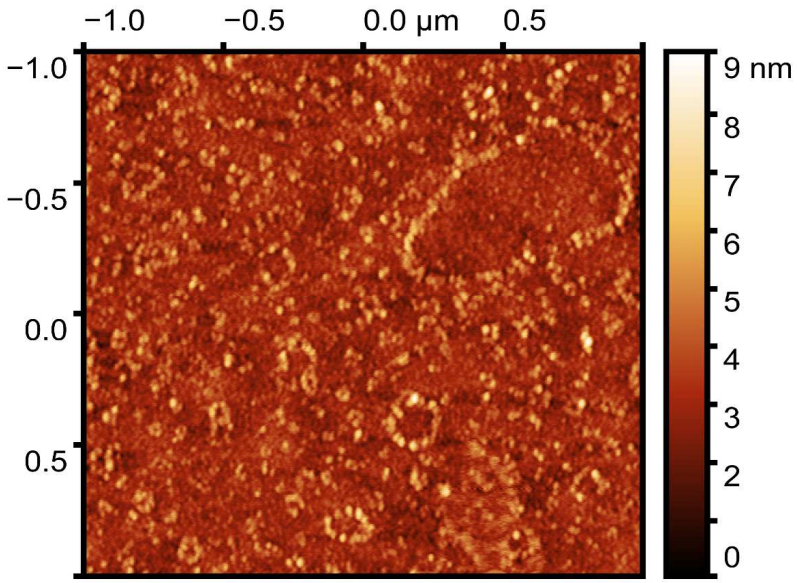

Figure 10– Image AFM of MoO_3:MoS_2 hybrid layer obtained after sulfidation 5 min at 220 °C.

Since we have seen that pure MoS_2 films after sulfidation exhibit some perturbations, we have proceeded to the visualization of hybrid MoO_3:MoS_2 layer sulfidized 5 min either at 220°C or at 330°C. It can be seen in **Figure.11** the film sulfidized at 220°C **(Figure 11 a)** is homogeneous, its appearance is similar to that shown by the AFM image, with small grains that sometimes appear as pseudo-circles. However, when the hybrid HTL is sulfidized at 330°C **(Figure 11 b)** disturbed lines are clearly visible all over the surface of the film. These different behaviors can be attributed to the fact that the sulfidation temperature is only 220° C for hybrid HTL, while it was 330 °C in the case of nearly pure MoS_2 films **(Figure. 4b).** Using smaller temperature during the sulfidation allows minimizing the thermal expansion mismatch between the substrate and the layer, which permits to avoid the apparition of the observed disturbed wrinkles in the films.

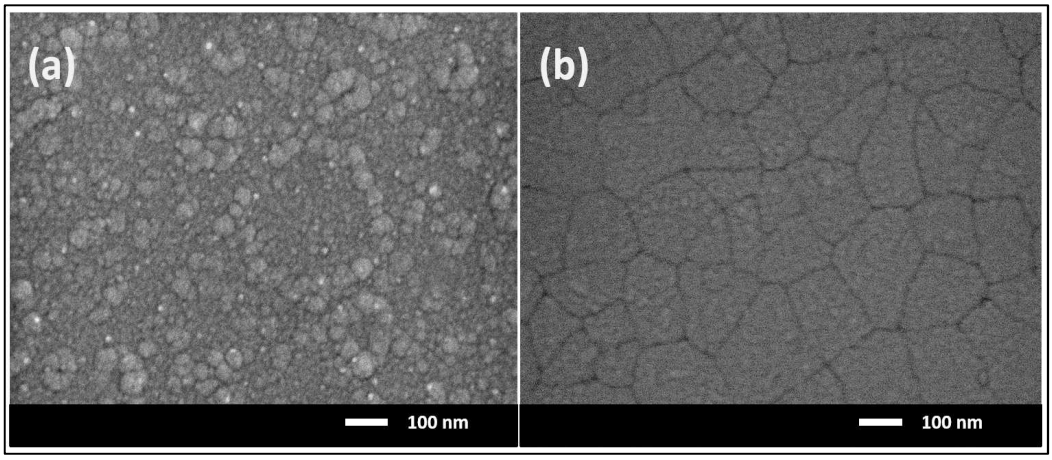

Figure 11– Surface visualization of a MoO_3 film sulfidized 5 min at 220 °C (a) and at 330°C (b)

After obtaining at quite low temperature homogeneous hybrid MoO_3:MoS_2 layers with composition supposed to be well suited for its use as HTL in OPVs, we have probed these hybrid layers in PHJ-OPVs.

3.3 MoO_3:MoS_2 hybrid layers as HTL in PHJ-OPVs.

For each deposition cycle we have introduced samples without any HTL, as reference OPV. Typical J-V characteristics are presented in **Figure 12**, while the results are summarized in **Table 3**.

Figure 12 presents the characteristics of an OPV without HTL, used as reference OPV, and that of an OPV with the optimum MoO_3:MoS_2 hybrid layer are visible. It is clear that the presence of the HTL improve the OPV performances. Without HTL the J-V characteristic is S-shaped, which is due to the bad band matching at the contact anode/AlPcCl [37]. On the other hand with MoO_3:MoS_2 HTL, the cell parameters, J_{sc} and FF are improved, which results in power conversion efficiency nearly double of that obtained without HTL.
It can be seen from **Table 3** that the OPV performance depends significantly on the MoO_3:MoS_2 HTL composition. We have shown that the MoO_3:MoS_2 ratio decreases when the sulfidation temperature increases (Table 2).

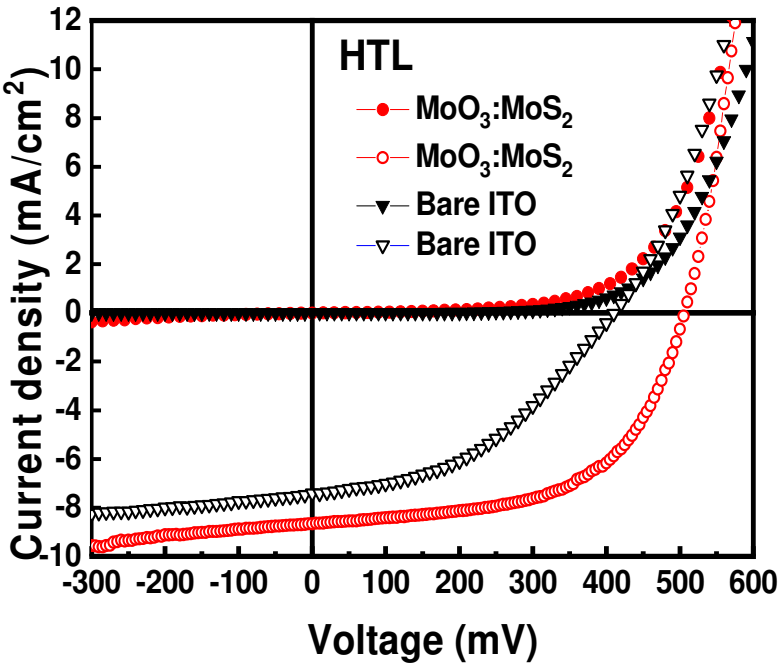

Figure 12– J-V characteristics of OPVs without HTL (▼) and with MoO_3:MoS_2 HTL (●), in dark (filled symbols) and under AM1.5 illumination (open symbols).

MoO_3 (%)	Mo^{5+} (%)	MoS_2 (%)	Annealing Temperature (°C)	V_{oc} (V)	J_{sc} (mA/cm^2)	FF (%)	η (%)
64	33	3	190	0.61	6.86	52	2.19
65	**30**	**5**	**210**	**0.50**	**8.66**	**57**	**2.49**
62	30	8	220	0.40	7.94	50	1.59
58	28	14	250	0.38	7.77	48	1.43
	Bare ITO			0.41	7.41	42	1.29

Table 3– Variation of the OPVs parameters with composition of the hybrid HTL MoO_3:MoS_2

If the performances of the OPVs increase with the MoS_2 concentration there is rapid saturation of this effect and, beyond 5% of MoS_2, the performances of cells degrade rapidly. J_{sc} and FF decrease beyond this MoS_2 critical concentration. About the open circuit voltage (V_{oc}), the introduction of the hybrid HTL increases significantly its value due to improvement of the band matching. Nevertheless, V_{oc} decreases systematically

when the MoS_2 concentration increases. This behavior limits the positive effect of the presence of MoS_2 in the hybrid HTL. This negative effect will be discussed below.

4. Discussion

In the present work, we show that, using MoO_3 thin films as precursor, it is possible to obtain in a short time (10 min) and at quite low temperature, (T > 340°C) for films with large majority of MoS_2 and 380°C for pure MoS_2 films, MoS_2 thin films using a mixed process: chemical vapor deposition (CVD) and rapid thermal annealing (RTA). This mixed technique makes it possible to obtain thick MoS_2 layers (20 – 25 nm) in a short time of 10 min and even only 5 min in the case of very thin layer (3 nm). Actually, classical CVD was already used to synthesize MoS_2, the starting material was often Mo thin films deposited by electron beam evaporation [38, 39], it was necessary to use far higher sulfidation temperature (750°C) to obtain homogeneous MoS_2 layer. That is in good agreement with our previous work [31] where we have shown that, starting from Mo thin films a minimum annealing temperature of 500°C was required to synthesize homogeneous MoS_2 thin films. Nevertheless, as shown by the present work, it is possible to grow homogeneous MoS_2 thin films at lowest temperature by using MoO_3 thin films as precursor. It was already shown that it was possible to grow MoS_2 from MoO_3 by sulfidation. For instance, starting form MoO_3 thin films, thick of 5 nm and 90 nm, deposited by reactive sputtering, MoS_2 thins films were grown by CVD, but for annealing temperature and duration being 400°C - 1h, 450°C – 1h, 550°C – 1h and 850°C – 15 min [40]. In the present work we were able to grow MoS_2 layer from MoO_3 layer at lower temperatures, T > 340°C for MoS_2 layers and T ≥ 200°C for MoO_3:MoS_2 hybrid layer. Such low temperatures were efficient due to the fact that with our CVD-RTA technique, the sulfur source is very close to the MoO_3 layer (4 cm) and the process takes place under the sulfur vapor (**Figure 2**), the reaction process being schematized in **Figure 13**. For the technique to be effective the P_{Sulfur}/P_{Oxygen} partial pressure ratio must be sufficiently high, here it is around 10^2 Pa. Others works propose small temperatures for MoS_2 synthesis, for instance 200°C by hydrothermal method, but the reaction process needs 24h to be effective [41].

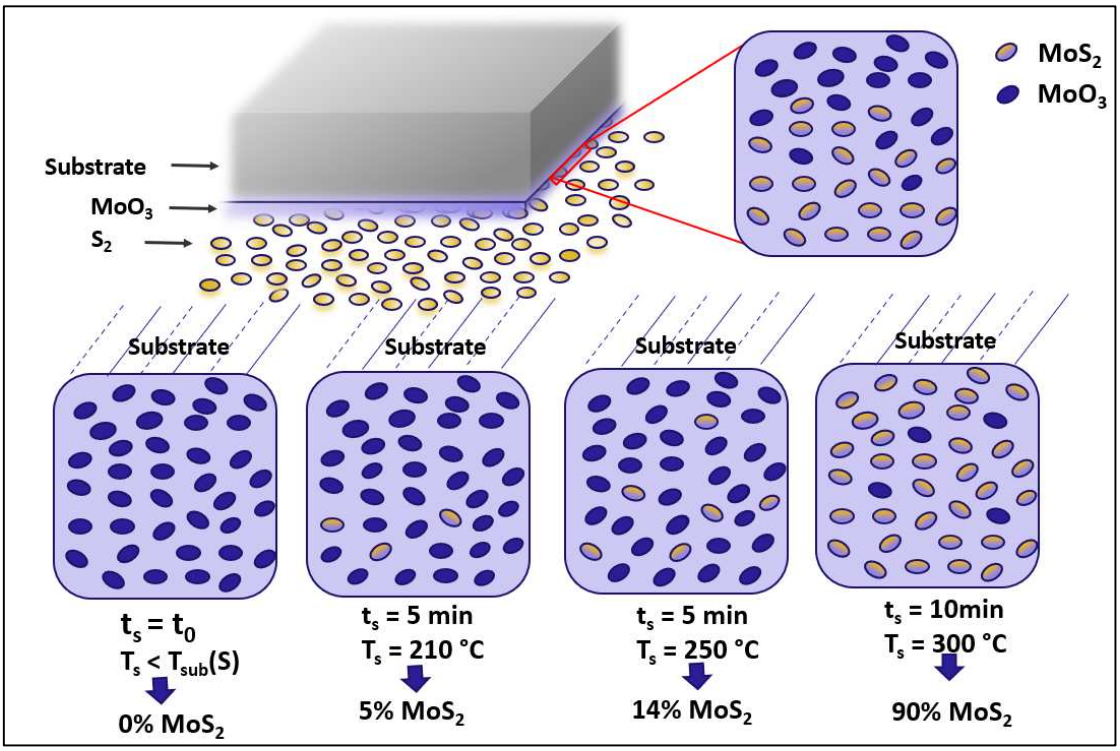

Figure 13– Schematization of the sulfidation process of the MoO_3 layers (T_{sub} is the sulfur sublimation temperature and T_s is the sulfidation temperature).

Nevertheless, it is known that the obtaining of MoS_2 films through MoO_3 sulfidation, involves the initial reduction of MoO_3 into MoO_2 under sulfur environment, followed by the sulfidation, which usually involves quite high temperature in order to avoid the presence of MoO_2 in the final film [10, 11, 7, 6, 3, 1]. In our case, lower temperatures are necessary, and we can wonder about the absence of oxide in our layers. First of all, concerning the XPS analysis, it should be noted that the signal corresponding to the indium appears weakly, whereas, as shown in Figure 3c, the signal due to MoO_3 has completely disappeared from the Mo3d spectrum, this confirms that there is no more MoO_3 even at the MoS_2/ITO interface. On the other hand, the signal corresponding to Mo^{4+} is present and it can correspond to MoS_2, but also to MoO_2. Nevertheless, following the literature, Mo^{4+} bonded to S^{2-} was observed at 229.4 and 232.5 eV [42, 43], while Mo^{4+} bonded to O^{2-} was located at 229.8 and 233.0 eV [42]. It turns out that our study shows that, after sulfidation, the measured bonding energies for $Mo(3d_{5/2})$ and $Mo(3d_{3/2})$ are situated at 229.3 eV and 232.4 eV respectively, which corresponds to Mo^{4+} bonded to MoS_2 following references [42, 43]. Nevertheless, in order to check more precisely the presence or not of oxide in our sulfurized films we have submitted our films to Raman analysis. Typical spectrum of our MoO_3 and MoS_2 films are shown in **Figure 14**. It can be seen that after deposition the spectrum obtained corresponds to amorphous MoO_3 (Figure 14) with some large band about 666 cm^{-1} (B_{2g}, B_{3g},the asymmetric stretching of the Mo–O–Mo bridge the 820 cm^{-1} (Ag, B_{1g}) the symmetric

stretch of the terminal oxygen atoms [44]. On the other hand, the presence of two prominent peaks located at 380 and 407 cm^{-1}, corresponding to the $E1_{2g}$ and A_{1g} modes for MoS_2, indicates that MoS_2 is obtained [45], while no peaks corresponding to MoO_3 or MoO_2 are visible.It can therefore be concluded from these studies that the presence of MoO_2 is unlikely, without however completely excluding it being given the limits of the sensitivities of the characterization techniques used."

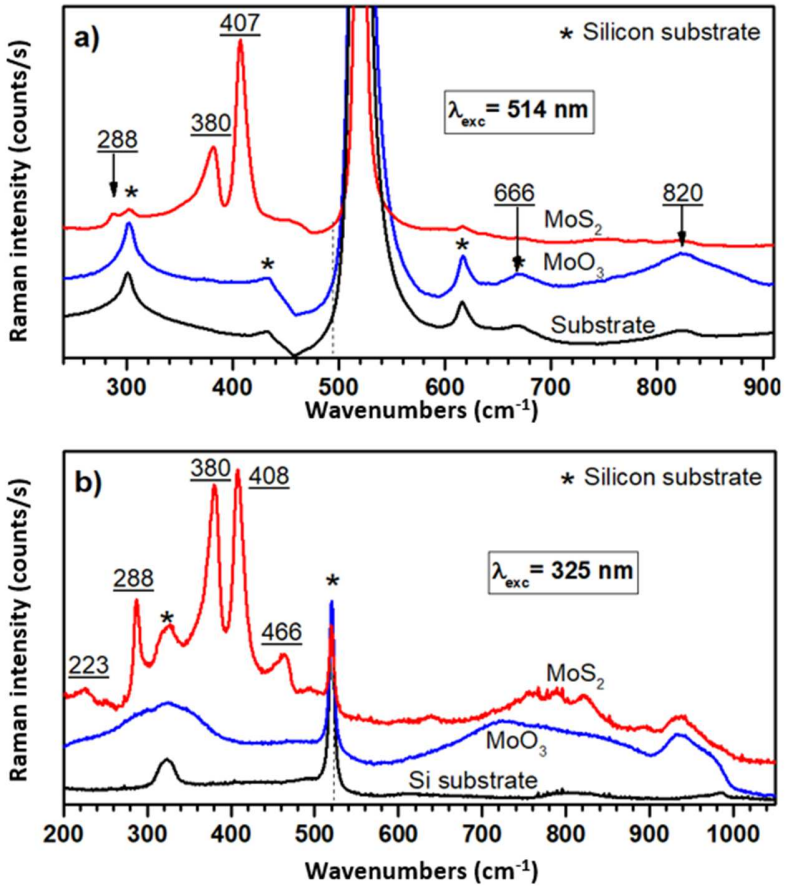

Figure. 14– Raman spectra (a) 514.5 nm excitation and (b) 325 nm excitation of thin films of MoO_3 (blue line) and MoS_2 (red line) taken in air at room temperature. Spectra of the Si substrate are also given for reference (black line)

About the improvement of OPVs efficiency by using MoO_3:MoS_2 hybrid HTL, it can be justified by looking more precisely some specific properties of MoO_3 and MoS_2. Among the known HTL, MoO_3 is often used. Actually, MoO_3 thin layers deposited by vacuum sublimation are oxygen deficient, making them type n, with a work function (W_F) of at least 5.9 eV – 5.3 eV in case of exposure to ambient air [42, 43]. Nevertheless, if MoO_3 is very efficient as hole collector layer, it does not behaves as an electron blocking layer [11, 44] due to its conduction band (4.93 eV) and valence band (8.49 eV) values [20]. Moreover, even if it is

semiconductor due to the presence of oxygen deficiencies, it remains fairly resistive (10^5 $\Omega^{-1}cm^{-1}$ [45]). All that means that OPVs, might be more efficient if an electron blocking layer with better conductivity was added to the MoO_3 HTL layer. It turns out that MoS_2 has the required energy levels to block electrons as it was already shown [10, 11, 46].

It is known that there is a large mismatch of the band structures of ITO/ED interface, which justifies the poor efficiency of the OPVs without HTL. When a MoO_3:MoS_2 hybrid HTL is introduced, J-V characteristics are improved, which results in a very significant improvement of the OPVs efficiency. Nevertheless, the trend is quickly reversed and when the concentration of MoS_2 is 6 or more, the efficiency of the OPVs decreases. In order to try to understand such behavior, knowing that the agreement of energy levels at the interfaces is very important we proceeded to the measurement of the work function, W_F, of MoO_3, MoS_2 and typical HTL using the technique PESA. For MoO_3 we have W_{FMoO3} = 5.31 eV. As said above, far higher value, 6.86 eV, was measured under ultra-high vacuum [44, 47]. Nevertheless, it was shown that this value decreases more than 1 eV when the MoO_3 layer is submitted to room air [42], which is the present case. Therefore we can consider that the measured value corresponds to the expected value. The value for MoS_2 is W_{FMoS2} = 4.95 eV. By comparison with previous studies which gives a value of 4.5 eV [10], this value is large, this may be due to some Mo oxidation [11], actually, the sample could be oxidized on the surface because it was not possible for us to make the PESA measurements immediately after the sulfidation of the layer.

In the case of the MoO_3:MoS_2 hybrid layer obtained after sulfidation 5 min at 220 °C we have $W_{FMoO3:MoS2}$ = 5.13 eV, which means that when the percentage of MoS_2 present in the hybrid layer increases W_F decreases slowly from the W_F value of MoO_3 to that of MoS_2. This result is in good agreement with previous studies that show that the presence of Mo^{6+} and Mo^{5+} , i.e., MoO_3 in the MoS_2 layers, increases the extraction work of the layer [11, 19]. The HOMO of AlPcCl being 5.35 eV, the agreement with MoO_3 is very good, while it is quite bad with MoS_2. The variation of W_F with the MoS_2 content in the hybrid HTL explains the results obtained in **Table 3**, while the presence of MoS_2 decreases the resistance of the HTL and blocks electrons it degrades the band matching. Using the hybrid buffer layer MoS_2:MoO_3, the idea was that such double anode buffer layer could allow cumulating the advantages of its both constituents. The MoS_2 blocks the electrons, while the high work function of MoO_3 induces a good band matching at the interface electron donor/anode. Moreover the high hole mobility of MoS_2 is favorable to improve J_{sc} and FF as it can be seen in **Table 3**. But this cumulative effect saturates rapidly. Such limitation is explained by the decrease of the W_F value of the hybrid HTL induced by MoS_2. Therefore, it is necessary to obtain the best tradeoff between the positive and negative effects of the presence of MoS_2 in MoO_3:MoS_2 HTL.

5. Conclusions

To improve the OPVs efficiency through the use of a MoO_3:MoS_2 HTL we propose in the present work, to control more simply its composition by using an original technique of sulfidation of a MoO_3 thin films. MoO_3 layers were deposited by vacuum sublimation, which means that they are oxygen deficient. Then, they were sulfidized by vacuum heat treatment under partial sulfur pressure. We first show that it is possible to obtain MoS_2 films by annealing MoO_3 films at 320°C for 10 min, pure MoS_2 films being obtained at 380°C. The low temperature needed for obtaining pure MoS_2 films demonstrates the high sulfidation efficiency of our CVD-RTA technique. CVD-RTA technique to be efficient, the P_{Sulfur}/P_{Oxygen} partial pressure ratio must be sufficiently high: $P_{Sulfur}/P_{Oxygen} = 10^2$. Then, we proceeded partial sulfidation of MoO_3 thinner layers (3 nm) to obtain MoO_3:MoS_2 hybrid layers, in order to cumulate the advantages of MoO_3, as a hole collecting layer and of MoS_2 as electron blocking layer. When a MoO_3:MoS_2 hybrid layer is introduced as HTL in OPV based AlPcCl/C_{60}, we have obtained a significant improvements of the OPV efficiency in the case of the HTL presents 5% of MoS_2. Nevertheless a small increase in the MoS_2 ratio induces a rapid saturation of this positive effect, which was explained by the decrease of the W_F of the MoO_3:MoS_2 hybrid HTL.

Acknowledgements

We gratefully acknowledge « le Centre National de la Recherche Scientifique et Technique (CNRST) » (PPR/2015/9 – Ministère Marocain), le Partenariat Hubert Curien (PHC) franco-marocain TOUBKAL project, under contract No. 41406ZC. We would like also to thank SFR MATRIX-Angers for PESA measurements.

Formatting of funding sources

This research did not receive any specific grant from funding agencies in the public, commercial, or not-for-profit sectors.

References

[1] G.Prasad and O.N. Srivastava, 1988, The high-efficiency (17.1%) WSe_2 photo- electrochemical solar cell, *J. Phys. D Appl. Phys*, vol. 21, no. 1028, 1988. https://doi.org/10.1088/0022-3727/21/6/029

[2] D. Tonti, F. Varsano, F. Decker, C. Ballif, M. Regula, and M. Remškar, 1997, Preparation and photoelectrochemistry of semiconducting WS_2 thin films, J. Phys. Chem. B, vol. 101, no. 14, pp. 2485–2490, 1997. doi: 10.1021/jp962550i.

[3] E. Gourmelon, O. Lignier, H. Hadouda, G. Couturier, J.C. Bernède, J.Tedd, J. Pouzet, J. Salardenne, 1997, MS_2 (M = W, Mo) photosensitive thin films for solar cells, Sol. Energy Mater. Sol. Cells, vol. 46, no. 2, pp. 115–121, 1997. doi: 10.1016/S0927-0248(96)00096-7.

[4] A. K. Geim and K. S. Novoselov, 2007, The rise of graphene, *Nat. Mater.*, vol. 6, pp. 183–191, 2007.

[5] H. Wang, C. Li, P. Fang, Z. Zhang and J.Z. Zhang, 2018, Synthesis, properties, and optoelectronic applications of two-dimensional MoS_2 and MoS_2-based heterostructures, Chem. Soc. Rev., vol. 47, no. 16, pp. 6101–6127, 2018. doi: 10.1039/c8cs00314a.

[6] N. Kondekar, P.P. Shetty, S.C. Wright, M.T. McDowell, 2021, In situ characterization of transformations in nanoscale layered chalcogenide materials: a review, Chem. Nano. Mat., vol. 7, pp. 1–16, 2021. https://doi.org/10.1002/cnma.202000575

[7] H. Schmidt, F. Giustiniano, and G. Eda, 2015, Electronic transport properties of transition metal dichalcogenide field-effect devices: surface and interface effects, *Chem. Soc. Rev.*, vol. 44, no. 21, pp. 7715–7736, 2015. https://doi.org/10.1039/C5CS00275C

[8] K. D. Rasamani, F. Alimohammadi, and Y. Sun, 2017, Interlayer-expanded MoS_2, Mater. Today, vol. 20, no. 2, pp. 83–91, 2017. https://doi.org/10.1016/j.mattod.2016.10.004

[9] C. K. Cheng and C. K. Hsieh, 2015, Electrochemical deposition of molybdenum sulfide thin films on conductive plastic substrates as platinum-free flexible counter electrodes for dye-sensitized solar cells, Thin Solid Films, vol. 584, pp. 52–60, 2015. https://doi.org/10.1016/j.tsf.2015.02.025

[10] J. K. Yun Mun Jin, Yong Jin Noh, Jun Seok Yeo, Yeong Jin Go, Seok In Na, Hyung Gu Jeong and D. Y. K. Sehyun Lee, Seok Soon Kim, Hye Young Koo, Tae Wook Kim, 2013, Efficient work-function engineering of solution-processed MoS_2 thin-films for novel hole and electron transport layers leading to high-performance polymer solar cells, J. Mater. Chem. C, vol. 1, no. 24, pp. 3777–3783, 2013. https://doi.org/10.1039/C3TC30504J

[11] P. Qin, G. Fang, W. Ke, F. Cheng, Q. Zheng, J. Wan, H. Lei and X. Zhao, 2014, In situ growth of double-layer MoO_3/MoS_2 film from MoS_2 for hole-transport layers in organic solar cell, J. Mater. Chem. A, vol. 2, no. 8, pp. 2742–2756, 2014. https://doi.org/10.1039/C3TA13579A

[13] Y. Z. Dongyang Zhu, Qiuyu Zhang, Xiaowei Li, 2021, Structural and electronic properties of MO_2/MS_2 heterojunctions and potential application in lithium-ion batteries," *J. Phys. Chem. C*, vol. 125, no. 8, pp. 4391–4396, 2021. doi: 10.1021/acs.jpcc.0c10349.

[14] L. Rapoport, N. Fleischer, and R. Tenne, 2005, Applications of WS_2 (MoS_2) inorganic nanotubes and fullerene-like nanoparticles for solid lubrication and for structural nanocomposites, *J. Mater. Chem.*, vol. 15, no. 18, pp. 1782–1788, 2005. https://doi.org/10.1039/B417488G

[15] X. Tong, E. Ashalley, F. Lin, H. Li, and Z. M. Wang, 2015, Advances in MoS_2-based field effect transistors (FETs), Nano-Micro Lett., vol. 7, no. 3, pp. 203–218, 2015. doi: 10.1007/s40820-015-0034-8.

[16] T. Corrales-Sánchez, J. Ampurdanés, and A. Urakawa, 2014, MoS_2-based materials as alternative cathode catalyst for PEM electrolysis, Int. J. Hydrogen Energy, vol. 39, no. 35, pp. 20837–20843, 2014. doi: 10.1016/j.ijhydene.2014.08.078.

[17] N. Balis, E. Stratakis, and E. Kymakis, 2016, Graphene and transition metal dichalcogenide nanosheets as charge transport layers for solution processed solar cells, Mater. Today, vol. 19, no. 10, pp. 580–594, 2016. https://doi.org/10.1016/j.mattod.2016.03.018

[18] F. Martinez-Rojas, M. Hssein, Z. El Jouad, F. Armijo, L. Cattin, G. Louarn, N.Stephant, M.A. del Valle, M. Addou, J.P. Soto, J.C. Bernède, 2017, $Mo(S_xO_y)$ thin films deposited by electrochemistry for application in organic photovoltaic cells, Mater. Chem. Phys., vol. 201, pp. 331–338, 2017. https://doi.org/10.1016/j.matchemphys.2017.08.021

[19] X. Gu , W. Cui , H. Li , Z. Wu , Z. Zeng , S-T. Lee, H. Zhang and B. Sun, 2013, A Solution-processed hole extraction layer made from ultrathin MoS_2 nanosheets for efficient organic solar cells, Adv. Energy Mater., pp. 1–7, 2013.
https://doi.org/10.1002/aenm201300549

[20] M. Shanmugam, C.A. Durcan and B.Yu, 2015, Multi-phase semicrystalline microstructures drive exciton dissociation in neat plastic semiconductors, J. Mater. Chem. C, vol. 3, no. 207890, pp. 10715–10722, 2015. https://doi.org/10.1039/C5TC02043C

[21] B. Radisavljevic, A. Radenovic, J. Brivio, V. Giacometti, and A. Kis, 2011, Single-layer MoS_2 transistors, Nat. Nanotechnol., vol. 6, no. 3, pp. 147–150, 2011. doi: 10.1038/nnano.2010.279.

[22] J. Tao, J. Chai, X. Lu, L.M. Wong, T.I. Wong, J. Pan, Q. Xiong, D. Chi and S. Wang, 2015, Growth of wafer-scale MoS_2 monolayer by magnetron sputtering, Nanoscale, vol. 7, no. 6, pp. 2497–2503, 2015. doi: 10.1039/c4nr06411a.

[23] M. Rakibuddin, M. A. Shinde, and H. Kim, 2020, Facile sol–gel fabrication of MoS_2 bulk, flake and quantum dot for electrochromic device and their enhanced performance with WO_3, *Electrochim. Acta*, vol. 349, p. 136403, 2020. doi: 10.1016/j.electacta.2020.136403.

[24] Q. Van Le, T. P. Nguyen, H. W. Jang, and S. Y. Kim, 2014, The use of UV/ozone-treated MoS_2 nanosheets for extended air stability in organic photovoltaic cells, Phys. Chem. Chem. Phys., vol. 16, no. 26, pp. 13123–13128, 2014. doi: 10.1039/c4cp01598c.

[25] M.M. Juvaid, M.S. Ramachandra Rao, 2020, Wafer scale growth of MoS_2 and WS_2 by pulsed laser deposition, Materials Today: Proceedings. https://doi.org/10.1016/j.matpr.2020.03.083

[26] M. Tsigkourakos, M. Kainourgiaki, E. Skotadis, Konstantinos P. Giannakopoulos, D. Tsoukalas, Yannis S. Raptisa, 2021, Capping technique for chemical vapor deposition of large and uniform MoS_2 flakes, Thin Solid Films, Volume 733, 1 September 2021, 138808. https://doi.org/10.1016/j.tsf.2021.138808

[28] J-C. Bernède, 2008, Organic photovoltaic cells: history, principle and techniques, J.Chil. Chem. Soc.,53, N°3 (2008) http://dx.doi.org/10.4067/S0717-97072008000300001

[29] Y. Lare, B. Kouskoussa, K. Benchouk, S. Ouro Djobo, L. Cattin, M. Morsli, F.R.Diaz, M.Gacitua, T.Abachi, M.A. dell Valle, F. Armijo Gaston, A.East, J.C.Bernède, 2011, Influence of the exciton blocking layer on the stability of the layered organic solar cells, Journal of Physics and Chemistry of Solids 72 (2011) 97-103. https://doi.org/10.1016/j.jpcs.2010.11.006

[30] A. Mohammed-Krarroubik, M. Morsli, A. Khelil, L. Cattin, L. Barkat, S. Tuo, Z. El Jouad, G. Louarn, M. Ghamnia, M. Addou, and J.C. Bernède, 2017, The influence of deposition rate on the properties of alpccl thin films and on the performance of planar organic solar cells, physica statut solidi (a), 2017. http://doi.wiley.com/10.1002/pssa.201700367

[31] H. Hadouda, J. Pouzet, J. C. Bernède, A. Barreau, 1995, MoS_2 thin film synthesis by soft sulfurization of a molybdenum layer", Materials Chemistry and Physics 42 (1995) 291-297. https://doi.org/10.1016/0254-0584(96)80017-4

[32] Gitti. L Frey, Kieran J. Reynolds, Richard H. Friend, Hagai Cohen, and Yishay Feldman, 2003, Solution-processed anodes from layer-structure materials for high-efficiency polymer light-emitting diodes, J. Am. Chem. Soc. 2003, 125, 19, 5998–6007. https://doi.org/10.1021/ja020913o

[33] Roxlo, C.B; Chianelli, R. R. ; Dckman, H.W. ; Ruppert, A. F. ; Wong, P.P. 1987, Bulk and Surface optical absorption in molybdenum disulfide, Journal of Vacuum Science & Technology A : Vacuum, Surfaces, and Films, Volume 5 Issue 4 July 1987, pp. 555-557. https://ui.adsabs.harvard.edu/abs/1987JVST....5..555R/abstract

[34] H. Hadouda, J. C. Bernède, J. Pouzet, R. Le Ny, 1997, Physicochemical characterization of MoS_2 films obtained by solid state reaction between the constituents of a multilayer Mo/S…/Mo/S structure, Mater. Sciences & Engineering B45 (1997) 9-16. https://doi.org/10.1016/S0921-5107(96)02011-9

[35] S.Y. Chiam, B. Dasgupta, D. Soler, M.Y. Leung, H. Liu, Z.E. Ooi, L.M. Wong, C.Y. Jiang, K.L. Chang, J. Zhang, 2012, Enhanced extraction rates through gap states of molybdenum oxide anode buffer, Energy Mater. Sol. Cells 99 (2012) 197. https://doi.org/10.1021/jp3114013

[36] J.Y. Sun, W. H. Tseng, S. Lan, S.H. Lin, P.C Yang, C.I. Wu, C.F. Lin, 2013, The effects of MoO_3 treatment on inverted PBDTTT-C:PC71BMsolar cells, Sol. Energy Mater. Sol. Cells 109 (2013) 178. https://doi.org/10.1016/j.solmat.2013.07.048

[37] P. Zamora, K. Kouskoussa, Z. El Jouad, K. El Assad Zemallach Ouari, K. Benchouk, J.C. Bernède, L. Cattin, 2020, New electron donor in planar heterojunction: optimization of the cells efficiency through the choice of the hole extracting layer, European Physical Journal Applied Physics (2020). https://doi.org/10.1051/epjap/2020190346

[38] Y. Zhan, Z. Liu, S. Najmaei, P. M. Ajayan, J.Lou, 2012, Large-area vapor-phase growth and characterization of MoS_2 atomic layers on SiO_2 substrate", Samll 2012, 8, 966-971. https://doi.org/10.1002/smll.201102654

[39] M. Shanmugam, Chris A. Ducan, B. Yu, 2012, Layered semiconductor molybdenum disulfide nano membrane based Schottky-barrier solar cells, Nanoscale, 2012, 4, 7399-7405, https://doi.org/10.1039/C2NR32394J

[40] A.R. Waite, S. Pacley, N. R. Gllavin, A. A. Voevodin, C. Muratore, 2018, Tailoring ultra-thin MoS_2 films via post-treatment of solid state precursor phases, Thin Solid Films 2018, 649, 177-186. https://doi.org/10.1016/j.tsf.2018.01.034

[41] G. Feng, A. Wei, Y. Zhao, J. Liu, 2015, Synthesis of flower-like MoS_2 nanosheets microspheres by hydrothermal method, J. Mater. Sci: Mater. Electron. https://doi.org/10.1007/s10854-015-3476-3

[42] H. Kang, J. S. Youn, I. Oh, K. Manavalan, and K. J. Jeon, "Controllable atomic-ratio of CVD-grown MoS_2-MoO_2 hybrid catalyst by soft annealing for enhancing hydrogen evolution reaction," Int. J. Hydrogen Energy, vol. 45, no. 3, pp. 1399–1408, 2020, doi: 10.1016/j.ijhydene.2019.11.066.

[43] A. A. Bortoti, A. de F. Gavanski, Y. R. Velazquez, A. Galli, and E. G. de Castro, "Facile and low cost oxidative conversion of MoS2 in α-MoO3: Synthesis, characterization and application," *J. Solid State Chem.*, vol. 252, no. January, pp. 111–118, 2017, doi: 10.1016/j.jssc.2017.05.006.

[44] B. C. Windom, W. G. Sawyer, and D. W. Hahn, "A raman spectroscopic study of MoS2 and MoO3: Applications to tribological systems," *Tribol. Lett.*, vol. 42, no. 3, pp. 301–310, 2011, doi: 10.1007/s11249-011-9774-x.

[45] S. Hao, B. Yang, and Y. Gao, "Chemical vapor deposition growth and characterization of drop-like MoS2/MoO2 granular films," *Phys. Status Solidi Basic Res.*, vol. 254, no. 4, pp. 1–7, 2017, doi: 10.1002/pssb.201600245.

[46] Irfan, H. Ding, Y. Gao, C. Small, D. Y. Kim, J. Subbiah, and F. So, 2010, Energy level evolution of air and oxygen exposed molybdenum trioxide films, Appl. Phys. Lett. 96 (2010) 243307. https://doi.org/10.1063/1.3454779

[47] L. Cattin, Y. Lare, M. Makha, M. Fleury, F. Chandezon, T. Abachi, M. Morsli, K. Napo, M. Addou, J. C. Bernède, 2013, Effect of the ag deposition rate on the properties of conductive transparent moo_3/ag/moo_3 multilayers. Solar Energy Materials & Solar Cells 117 (2013) 103-109. https://doi.org/10.1016/j.solmat.2013.05.026

[48] J. Meyer, S. Hamwi, M. Kröger, W. Kowalski, T. Riedl, A. Khan, 2012, Transition metal oxides for organic electronics: energetics, device physics and applications, Adv. Mater 24 (2012) 5408. https://doi.org/10.1002/adma.201201630

[49] L. Cattin, F. Dahou, Y. Lare, M. Morsli, R. Tricot, K. Jondo, A. Khelil, K. Napo, J.C. Bernède, 2009, MoO_3 surface passivation of the transparent anode in organic solar cells using ultra-thin films, J. Appl. Phys. 105 (2009) 034507. https://doi.org/10.1063/1.3077160

[50] Bourgeteau, D. Tondelier, B. Geffroy, R. Brisse, R. Cornut, V. Artero, B. Jousselme, 2015, Enhancing the Performances of P3HT:PCBM-MoS_3-Based H_2-Evolving Photocathodes with Interfacial Layers, ACS Appl. Mater. Interfaces 7 (30) (2015) 16395. https://doi.org/10.1021/acsami.5b03532

[51] M. Kröger, S. Hamwi, J. Mayer, W. Kowalski, 2009, Role of the deep-lying electronic statesof MoO_3 in the enhancement of hole-injection in organic thin films, Appl. Phys. Lett. 95, 123301(2009). https://doi.org/10.1063/1.3231928

Graphical abstract